Proceedings of the ASME 2023 42nd International Conference on Ocean, Offshore and Arctic Engineering
OMAE2023
June 11–June 16, 2022, Melbourne, AU

OMAE2023-100845

ANALYTICAL MODEL OF NON-LINEAR LOAD REDUCTION DEVICES FOR CATENARY MOORINGS

Oscar Festa[1], Susan Gourvenec[1], Adam Sobey[1,2]

[1] Faculty of Engineering and Physical Sciences, University of Southampton, UK
[2]Data-Centric Engineering, The Alan Turing Institute, UK

ABSTRACT

Load reduction devices are extensible components which can be installed along mooring lines to reduce peak loads and fatigue damage in the mooring system. This has the potential to reduce risk of failure for Floating Offshore Wind Turbine (FOWT) mooring systems, and can provide significant reductions to the overall material, handling and installation costs of a FOWT project. Various load reduction device concepts exist, including ballasted pendulums, thermoplastic springs and hydraulic dampers, all of which are designed to exhibit a non-linear load-extension behaviour: lower stiffness in the operational strain range to reduce loads, and higher stiffness at high strain. These devices are becoming an increasingly common consideration for FOWT mooring systems, and are pushing traditional analysis and design methods to readily incorporate non-linearity. Well-established static catenary equations, used to define mooring tension-offset profiles, only account for linear elasticity such that capturing non-linear response typically requires finite element modelling. This paper presents an alternative through parameterising equations for three different non-linear load-extension curves and incorporating them into the existing catenary equations. For a given non-linear load-extension curve and length of load reduction device, the resulting analytical model can be solved quasi-instantaneously using Newton-Raphson or Newton-Krylov iterations to give vertical and horizontal mooring line tensions and thus strain of the device. Results from the new analytical model are compared with finite element predictions showing agreement to within 1%. The analytical model can be solved for any two unknowns, such that optimal load reduction device length and stiffness can be determined instantaneously given maximum environmental load and allowable offset. The new analytical equations are implemented into a graphical app, which allows the user to input any load reduction device parameters and visualise the resulting mooring system's geometry and tension-offset profile.

Documentation for `asmeconf.cls`: Version 1.31, July 4, 2023.

1. INTRODUCTION

1.1 Motivation for compliant FOWT mooring design

Up to 80% of worldwide offshore wind resources are in water depths greater than 60 m [1], where traditional fixed-bottom wind farms are not economically viable. In these deeper waters, offshore wind turbines must be deployed on floating structures, connected to the seabed via mooring lines and anchors. Mooring systems are designed to ensure station-keeping of the floating structure: they maintain the structure within an acceptable distance from its reference position. Station-keeping requirements for Floating Offshore Wind Turbines (FOWTs) are often more lenient than for oil & gas installations [2] and are primarily constrained by the motion of the electrical power cable [3].

Designing a mooring system involves finding a balance between stiffness and compliance to fit the station-keeping requirements [4]. A stiffer mooring system will maintain the floating structure closer to its reference position, at the expense of high loads on the mooring lines and anchors. A compliant mooring system will allow more motion of the floating structure in response to environmental loads, reducing forces in the mooring line and anchor, in turn allowing for smaller, cheaper anchors and a reduced chance of mooring line failure (Table 1). As FOWT farms require large amounts of structures to be moored to the seabed, reducing mooring and anchoring costs per unit through compliant moorings can lead to significant overall savings.

TABLE 1: EFFECT OF COMPLIANCE ON FOWT SYSTEM

Mooring design:	stiff	compliant
Platform displacements	–	+
Mooring and anchor loads	+	–
Mooring and anchor cost	+	–

In response to the incentive to reduce the cost of FOWT moorings, various means of adding compliance to mooring systems have been developed, in particular in the form of load reduction devices (LRDs). Current concepts include the Exeter Intelligent

Mooring System (IMS), (Fig.1a) [5], the Dublin Offshore LRD (DO), (Fig.1b) [6], and the Technology for Ideas Seaspring (TFI), (Fig.1c) [7]. These devices are incorporated into a mooring line, typically close to the fairlead, and can provide high levels of compliance (extensibility) without compromising breaking strength [8]. For the same breaking strength, typical synthetic ropes cannot achieve such low elastic stiffness. The DO and TFI devices are passive, whereas the IMS is 'active' as it can change stiffness curve in operation. Thus, two curves are considered for the IMS device, which correspond to the upper and lower bound stiffness for the given configuration.

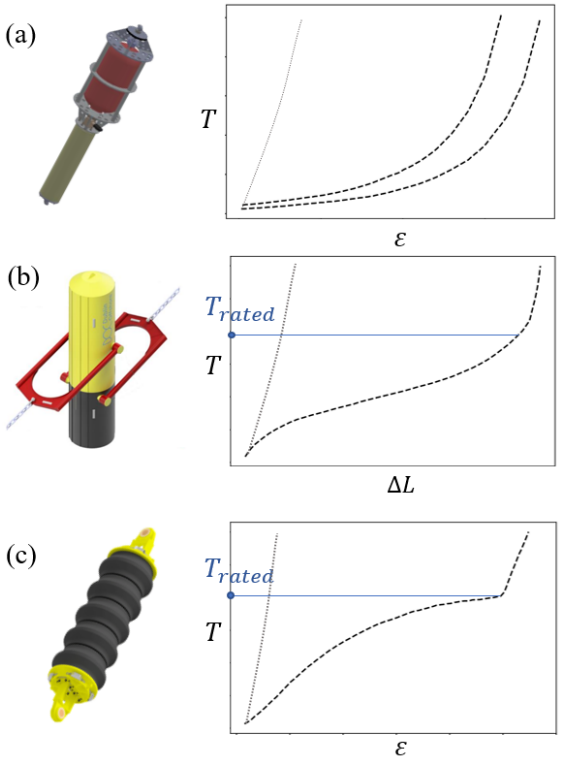

FIGURE 1: LRD TECHNOLOGIES AND ASSOCIATED STIFFNESS CURVES: (A) IMS [5], (B) DO [6], (C) TFI [7] . POLYESTER ROPE STIFFNESS SHOWN WITH GRAY DOTTED LINE FOR COMPARISON

These devices have highly non-linear stiffness curves, which can be tailored to fit the specific loading conditions and mooring arrangement (Fig. 1). These non-linear stiffness curves have a compliant range over which the LRD is intended to operate to effectively reduce mooring line tension. The curves then exhibit higher stiffness at high strain when they reach their rated tension T_{rated}, i.e., once all the compliance has been exhausted. Graphical representation of the rated tension is shown for DO and TFI in Figure 1. The key to designing a mooring system with a LRD is to ensure the device operates in its compliant range as much as possible, meaning the LRD is generally designed such that the maximum tension in the device stays below T_{rated}. The optimal length of the LRD should then be determined to ensure the extension provided does not exceed station-keeping constraints. Current approaches to finding this optimal length and rated tension involve time-consuming iterations of Finite Element (FE) analyses. The aim of this paper is to propose an analytical model of catenary moorings with LRDs, which can be used for efficient quasi-static design of an LRD mooring system.

1.2 Quasi-static mooring system design

If all dynamic mooring effects (damping, inertia) are ignored, and the system is assumed to be static at a given instant t, the geometry of the mooring line can be solved analytically as a function of the fairlead coordinates and the physical parameters of the mooring line. This constitutes the quasi-static mooring analysis, which is typically the first step in mooring system design [9]. The quasi-static analysis is useful for determining the tension-offset response of a mooring system, which informs designers of the restoring force provided by the system in response to displacement of the fairlead.

For neutrally buoyant taut moorings, the relationship between fairlead coordinates and restoring forces is trivial: the mooring line adopts a straight line between the fairlead and anchor, and the tension-offset of the system corresponds directly to the material stiffness of the mooring line [10]. This relationship is more complex for catenary moorings, as the catenary configuration (i.e., weight of suspended line) is controlled by tension, leading to a non-linear tension-offset profile. This is captured by the catenary mooring equations, which define the fairlead coordinates x_f and z_f as a function of the fairlead restoring forces H_f and V_f [11] and the mooring line length L, stiffness EA and unit weight w (Fig. 4). For a line partially resting on a friction-less seabed:

$$x_f(H_f, V_f) = L - \frac{V_f}{w} + \frac{H_f}{w} \cdot \ln\left[\frac{V_f}{H_f} + \sqrt{1 + \left(\frac{V_f}{H_f}\right)^2}\right] + \frac{H_f L}{EA} \tag{1a}$$

$$z_f(H_f, V_f) = \frac{H_f}{w} \cdot \left[\sqrt{1 + \left(\frac{V_f}{H_f}\right)^2} - 1\right] + \frac{V_f^2}{2EAw} \tag{1b}$$

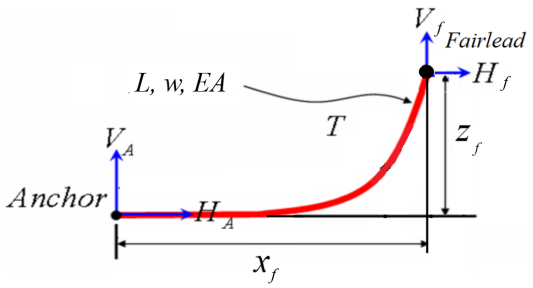

FIGURE 2: PROFILE VIEW OF SIMPLE CATENARY MOORING LINE

The system of equations 1a & 1b can then be solved for any two unknowns. However, this is only valid for a homogeneous mooring line (i.e. full chain), and the stiffness term EA must be linear. As such, these equations cannot be used for analysis of a mooring system with a non-linear LRD. Other publications have presented equations for multi-segmented catenary mooring lines with a non-linear stiffness segment, in particular for polymer rope applications [10]. The non-linear stiffness is expressed in simple

power law form, where the strain ε is given as a function of axial load T and constants p and q :

$$\varepsilon = pT^q \tag{2}$$

The power law form offers a good fit for material stiffness of typical synthetic polymer ropes, but this does not match the LRD stiffness curves as shown in Figure 1.

Since no analytical solution is available, current approaches to modelling moorings with LRDs include discretisation of the mooring lines and/or piece-wise linear interpolation of the non-linear stiffness curves. Commercial software such as Orcaflex is typically used for dynamic modelling of LRDs [12], which uses linear interpolation between consecutive points of the user-defined non-linear stiffness curve. LRDs have also been modelled with the open-source lumped-mass modelling software Moordyn, which also uses linear interpolation of the stiffness curve [7].

This paper presents continuous functions which model the non-linear stiffness curves of the LRD devices shown in Figure 1. These functions are then combined with the existing equations for catenary moorings, to create a static analytical model of catenary moorings with LRDs. This requires no discretisation or stiffness interpolation, and as such provides a quicker approach to obtain the mooring geometry and restoring forces based on any input mooring properties and LRD parameters (rated tension, curve shape, LRD length). The analytical model can then be used to find optimal LRD parameters for a given water-depth, mean environmental load, and offset constraint.

2. METHOD

This paper employs an analytical approach to mooring systems modelling. Firstly, a 2-segment formulation for a catenary mooring line with a linear-stiffness LRD at the fairlead is presented based on established equations. This formulation is then adapted with various non-linear stiffness functions, to form a set of equations for a chain catenary line with non-linear LRDs. These are solved using numerical root-finding methods, in particular the Newton-Raphson method [13], implemented in Python. Commercial FE software Flexcom is then used to validate the results obtained from the analytical equations. The validated analytical model is then applied to initial quasi-static design of an LRD. A structural overview of the methodology of the paper is shown in Fig 3.

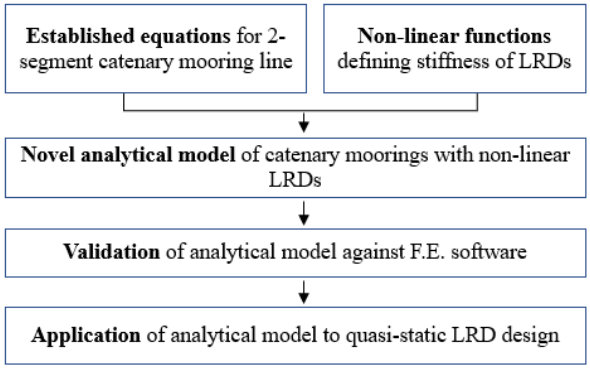

FIGURE 3: METHODOLOGY FOR THE ANALYTICAL SOLUTION

3. DEVELOPMENT OF ANALYTICAL MODEL

3.1 Catenary equations for linear-stiffness LRDs

The static catenary equations 1a & 1b apply to a catenary line formed of a unique, homogeneous segment, with material properties defined by a single value of stiffness EA and apparent weight in water per unit length w. This section presents an adapted formulation for a mooring line with two distinct segments: one segment for the chain catenary line and one segment for a linear stiffness LRD at the fairlead (Fig. 4). This linear LRD formulation is then used as the starting point for the next section, which presents the equation for non-linear stiffness LRDs.

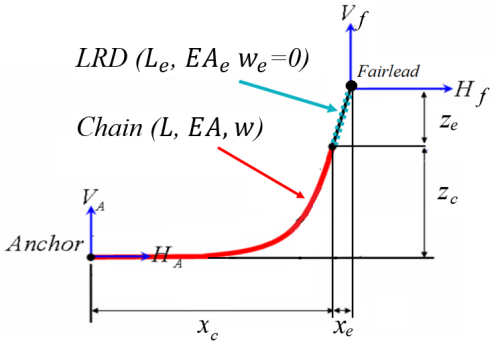

FIGURE 4: PROFILE VIEW OF THE MULTISEGMENT LINE

The static multi-segment mooring analysis approach is well-documented in literature [10]. For a catenary line composed of n segments of line, the fairlead coordinates (x_f, z_f) are given as a sum of the horizontal and vertical components of each segment:

$$x_f = \sum_{i=1}^{n} x_i \tag{3a}$$

$$z_f = \sum_{i=1}^{n} z_i \tag{3b}$$

Where the coordinates of the extremities of the i^{th} segment x_i and z_i are each defined by the catenary equations in their own coordinate system, with the origin at the start of the segment (starting from the anchor).

If the LRD is modelled as a simple non-linear spring segment, and assumed to be near-neutrally buoyant in water, which is typically the case of the IMS and DO technologies [5][6], this means the spring is subjected to constant tension throughout its length, thus adopting a straight line rather than a catenary shape. For a linear stiffness LRD, its extension ΔL_e is based on Hooke's law, where the tension-strain profile is a straight line passing through the origin and a single point EA. The coordinates of the horizontal and vertical extremities of the LRD segment (x_e, z_e) are then given by:

$$x_e = \frac{H_f l_e}{\sqrt{H_f^2 + V_f^2}} + \frac{H_f L_e}{EA_e} \tag{4a}$$

$$z_e = \frac{V_f l_e}{\sqrt{H_f^2 + V_f^2}} + \frac{V_f L_e}{EA_e} \tag{4b}$$

Where the left-hand terms represent the horizontal (4a) or vertical (4b) projections of the unstretched length L_e of the LRD, and the right-hand term represents the elongation of the LRD, obeying Hooke's law.

According to the multisegment theory from equations 3a & 3b, equations 4a & 4b can be added to the chain catenary equations to give the coordinates of the fairlead (x_f, z_f) as a function of the restoring forces (H_f, V_f):

$$x_f(H_f,V_f) = L - \frac{V_f}{w} + \frac{H_f}{w}\cdot\ln\left[\frac{V_f}{H_f} + \sqrt{1+\left(\frac{V_f}{H_f}\right)^2}\right] + \frac{H_f L}{EA} + \frac{H_f L_e}{\sqrt{H_f^2+V_f^2}} + \frac{H_f L_e}{EA_e} \tag{5a}$$

$$z_f(H_f,V_f) = \frac{H_f}{w}\cdot\left[\sqrt{1+\left(\frac{V_f}{H_f}\right)^2} - 1\right] + \frac{V_f^2}{2EAw} + \frac{V_f L_e}{\sqrt{H_f^2+V_f^2}} + \frac{V_f L_e}{EA_e} \tag{5b}$$

3.2 Catenary equations for non-linear stiffness LRDs

To replace the Hookean extension term in equations 4a & 4b, the non-linear extension of the LRD must be defined as a function of the force applied at its extremities. This means determining the function ε which gives the LRD strain for any value of axial mooring line tension T, where T is the resultant of the horizontal and vertical mooring line forces H_f and V_f :

$$\varepsilon(T) = \varepsilon(\sqrt{H_f^2+V_f^2}) = \frac{\Delta L_e}{L_e} \tag{6}$$

Equations analogous to 5a and 5b can be obtained by substituting the Hookean extension term (the final term in equations 5a & 5b) with the non-linear strain function ε, giving:

$$x_f(H_f,V_f) = L - \frac{V_f}{w} + \frac{H_f}{w}\cdot\ln\left[\frac{V_f}{H_f} + \sqrt{1+\left(\frac{V_f}{H_f}\right)^2}\right] + \frac{H_f L}{EA} + \frac{H_f L_e}{\sqrt{H_f^2+V_f^2}}(1+\varepsilon(T)) \tag{7a}$$

$$z_f(H_f,V_f) = \frac{H_f}{w}\cdot\left[\sqrt{1+\left(\frac{V_f}{H_f}\right)^2} - 1\right] + \frac{V_f^2}{2EAw} + \frac{V_f L_e}{\sqrt{H_f^2+V_f^2}}(1+\varepsilon(T)) \tag{7b}$$

These equations are valid for an extensible section located at the fairlead, attached to a homogeneous catenary mooring line with a portion resting on the seabed (i.e. no vertical loading on the anchor), where seabed friction is neglected. An analogous expression can also be derived for non-buoyant taut and semi-taut moorings where vertical anchor loading is non-zero, based on the equations for a fully-suspended line [11].

Equations 4a & 4b assume that the extensible section is neutrally buoyant in seawater. This is a valid assumption for the IMS and DO devices, but the TFI device has a non-negligible weight in water [7]. This means the upper extremity of the LRD is subjected to additional tension due to self-weight of the device, with a difference in vertical tension between the two extremities equal to $L_e w_e$ where L_e is the length of the device and w_e is its wet weight per unit length. Due to this difference in tension, the strain of the LRD is not constant along its length, and requires an integral to compute analytically. As a simpler approximation, the tension can be assumed to be constant throughout the LRD, taking the value of the tension at its midpoint, which is subjected to half of the self weight of the LRD: $\frac{1}{2}L_e w_e$. With this assumption, the strain in the device given by Equation 6 can be redefined as:

$$\varepsilon(T) = \varepsilon\left(\sqrt{H_f^2 + (V_f - \frac{1}{2}L_e w_e)^2}\right) \tag{8}$$

The chain section of the line, which is below the LRD, is not subjected to the additional vertical tension component. Thus, we define the component of vertical tension at the top chain as V_{tc} which does not include the self weight, and is given by $V_{tc} = V_f - L_e w_e$. The full expression is then given by:

$$x_f(H_f,V_f) = L - \frac{V_{tc}}{w} + \frac{H_f}{w}\cdot\ln\left[\frac{V_{tc}}{H_f} + \sqrt{1+\left(\frac{V_{tc}}{H_f}\right)^2}\right] + \frac{H_f L}{EA} + \frac{H_f L_e}{\sqrt{H_f^2+(V_f-\frac{1}{2}L_e w_e)^2}}(1+\varepsilon(T)) \tag{9a}$$

$$z_f(H_f,V_f) = \frac{H_f}{w}\cdot\left[\sqrt{1+\left(\frac{V_f}{H_f}\right)^2} - 1\right] + \frac{V_f^2}{2EAw} + \frac{(V_f-\frac{1}{2}L_e w_e)L_e}{\sqrt{H_f^2+(V_f-\frac{1}{2}L_e w_e)^2}}(1+\varepsilon(T)) \tag{9b}$$

3.3 Continuous functions for LRD stiffness curves

Adapting the general-form equations 7a & 7b or 9a & 9b to a specific LRD technology requires determining the function $\varepsilon(T)$which gives LRD strain as a function of axial tension T. In this section, functions have been derived for the three curve types shown in Figure 1. These functions are mostly based on the Ramberg-Osgood model, which is typically used to define non-linear stress-strain relationships. The original model defines stress as a function of strain and 3 parameters [14]. In this case, the model is used only in its mathematical sense, and the form is reversed to define strain ε as a function of axial tension T such that it can be incorporated into the catenary equations. This adaptation of the basic-form Ramberg-Osgood model can be given as:

$$\varepsilon(T) = \frac{aT}{(1+(\frac{aT}{c})^n)^{\frac{1}{n}}} \tag{10}$$

Where a, c and define the shape of the curve (Fig. 5).

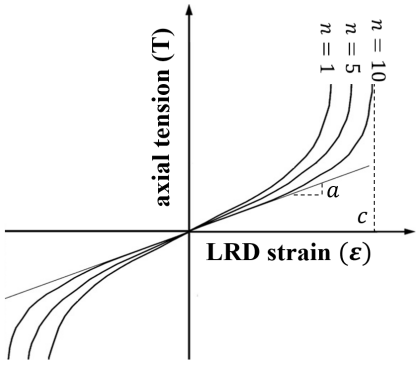

FIGURE 5: BASIC-FORM RAMBERG-OSGOOD CURVE

The basic form equation of the Ramberg-Osgood model given in Equation 10, does not directly fit all of the LRD devices identified in Figure 1, in particular the TFI and DO LRDs which require additional terms and parameters. These variations of the basic form equation are described in the following subsections.

Exeter IMS

The curve of the IMS is the closest fit to the Ramberg-Osgood model, with the exception of the curve not passing through the origin due to variable pre-load in the device [5]. An additional parameter b is introduced, which shifts the curve along the x-axis from the origin, such that the overall equation is given by:

$$\varepsilon_{IMS}(T) = \frac{aT - b}{(1 + (\frac{aT-b}{c})^n)^{\frac{1}{n}}} \tag{11}$$

Where b/a is the pre-tension, c is the asymptotic strain, and n is a parameter defining the rate at which the curve reaches its asymptotic strain, as shown in Figure 5. The value of n can be found if the rated tension required at a specific value of strain is known. The parameters of Equation 11 are fitted to two example supplier curves [5], using a simple linear regression algorithm, and the resulting curve fits are plotted in Figure 6. The values of each fitted parameter are given in Table 2, for curves A and B.

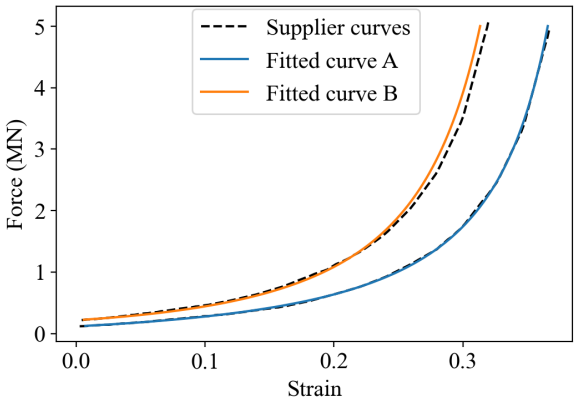

FIGURE 6: IMS STIFFNESS CURVES FROM SUPPLIER PUBLICATION [5], AGAINST FITTED CURVE FROM EQ. 11

TABLE 2: IMS FITTED PARAMETERS FOR EQ. 11

Parameter	fitted value (A)	fitted value (B)
a	0.958	0.837
b	0.113	0.183
c	0.426	0.396
n	0.834	0.728

Dublin Offshore LRD

To obtain an expression of the DO curve, the base curve from Figure 5 is translated with an additional parameter b, as with the IMS fit. However, the curve must pass through the origin, which is not the case of the IMS curve in Eq. 11, which passes through the point $[0, \varepsilon(0)]$, where $\varepsilon(0)$ given by:

$$\varepsilon_{IMS}(0) = \frac{-b}{(1 + (\frac{b}{c})^n)^{\frac{1}{n}}} \tag{12}$$

To ensure that the DO curve passes through the origin, the term shown in Eq. 12 is subtracted from Eq. 11, giving an expression of $\Delta L_{Dublin}(T)$ (Eq. 13). The shape factor n, which defines the rate at at which the function reaches its asymptote, is fixed to $n = 2$. The parameters a, b and c of Equation 13 are fitted to the example curve from supplier documentation [6] using linear regression, resulting in the curve fit shown in Figure 7. The values of each fitted parameter for this curve are given in Table 3.

$$\Delta L_{Dublin}(T) = \frac{aT - b}{(1 + (\frac{aT-b}{c})^2)^{\frac{1}{2}}} + \frac{b}{(1 + (\frac{b}{c})^2)^{\frac{1}{2}}} \tag{13}$$

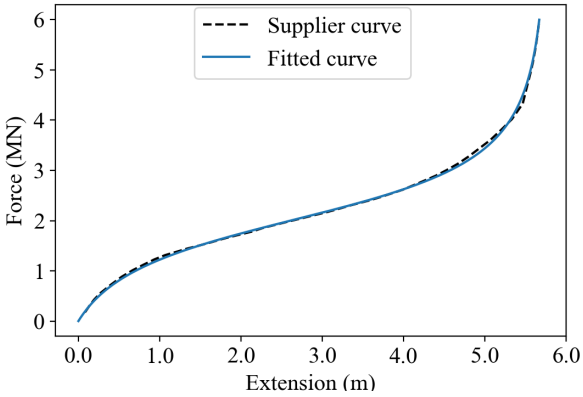

FIGURE 7: DO STIFFNESS CURVE FROM SUPPLIER PUBLICATION [6], AGAINST FITTED CURVE FROM EQ. 13

In Eq. 13, parameter a is related to the rated tension of the device and c is related to the asymptotic extension of the device. These parameters can also be linked to physical dimensions of the device, based on supplier documentation [6]. As opposed to the IMS and TFI devices which are spring-like, the DO LRD extends by rotating under loading (Fig. 1b). Thus, extension $\Delta L(T)$ is used rather than the strain term $\varepsilon(T)$. When incorporated into the final system of static equations 7a & 7b, the

TABLE 3: DO FITTED PARAMETERS FOR EQ. 13

Parameter	fitted value
a	7.500
b	7.432
c	2.568

length of device Le can then be based on the starting distance between the two hinge points. It should also be noted that Eq 13 is only valid for a fixed mooring line angle. The line angle affects the magnitude of the moment generated by the mooring line on the LRD hinges, in turn changing the shape of the stiffness curve. A more complete expression is given in the published code [15], which captures the effect of the line angle, and relates the curve parameters to physical dimensions of the LRD.

TFI Seaspring

The TFI stiffness curve (Fig. 1b) is complex to model with a continuous function due to the sudden stiffness increase at $T = T_{rated}$. The required function deviates more significantly from the base Ramberg-Osgood model, in three ways: 1. Parameter c is subtracted to the denominator of the first term to create the sudden gradient change; 2. An additional parameter k is introduced to factorise the whole expression, such that the rated strain of the curve can be directly adjusted without changing the other parameters; 3. An additional term is introduced, function of a new parameter d, in an attempt to better match the final phase stiffness. The resulting expression is given in Eq. 14, with the associated curve fit is shown in Figure 8, and the fitted parameter values given in Table 4.

$$\varepsilon_{TFI}(T) = k \cdot \left(\frac{a(eT-f)-b}{1+[a(eT-f)-b-c]^2} + \frac{af+b}{1+[-af-b-c]^2} + d\sqrt{a(eT-f)} - d\sqrt{-af} \right) \tag{14}$$

The fit is accurate up to, and including, the sudden increase in stiffness at $T = T_{rated}$. . Accurate modelling of the response past this point is not crucial, as in practice the device should not be operating above T_{rated}. Although the expression is complex, only parameters k and e are required to parameterise the rated tension and strain. Any value of rated tension T_{rated} can be obtained by varying parameter e, and any value of rated strain $\varepsilon(T_{rated})$ can be obtained by varying parameter k.

For each LRD, the derived non-linear stiffness function is substituted for the $\varepsilon(T)$ term in the general form equations (7a & 7b, 9a & 9b), with the resulting systems of equations forming the analytical model. This model can be solved for the vertical and horizontal restoring forces H_f and V_f at the fairlead, for any fairlead coordinates x_f and z_f, by employing numerical root-finding methods. All LRD stiffness functions and resulting mooring equations are fully differentiable over their domain. This means the system can be solved with a Newton-Rhapson scheme with analytical Jacobians, providing fast and robust computation.

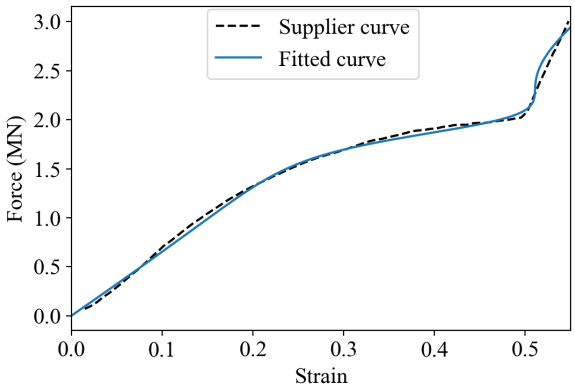

FIGURE 8: TFI STIFFNESS CURVE FROM SUPPLIER PUBLICATION [7], AGAINST FITTED CURVE FROM EQ. 14

TABLE 4: TFI FITTED PARAMETERS FOR EQ. 14

Parameter	fitted value
a	1.238×10^{-2}
b	2.119×10^{2}
c	7.516×10^{-1}
d	1.149×10^{1}
e	2.405×10^{2}
f	-1.672×10^{5}
k	1.379×10^{-1}

4. VALIDATION OF ANALYTICAL MODEL

The analytical model was then validated against results obtained from the commercial FE software Flexcom, which discretises the mooring line and interpolates the stiffness from a set of force-strain points. The validation was performed by comparing quasi-static tension-offset profiles for each of the LRD concepts. To obtain the quasi-static tension-offset profile, the horizontal fairlead coordinate x_t is gradually displaced along the horizontal axis parallel to the mooring line, and the analytical model is used to calculate the resultant fairlead tension T from the fairlead forces H_f and V_f at every step. This is depicted graphically in Figure 9. This figure was obtained using a graphical app built on Python, based on the analytical model, which enables visualisation of the geometry of a mooring system with any LRD parameters [15].

The properties of the mooring system used are identical to those of the OC4 Phase II mooring system [16], with the exception of the water depth which is set to 150 m rather than 200 m, to make the mooring system more sensitive to the LRD. These properties are summarised in Table 5. For each LRD concept, the stiffness curve parameters are taken from the curve fits shown in section 3.3 and the LRD lengths are set such that they all exhibit 5 m of extension at $T_{rated} = 2MN$. This rated tension was chosen arbitrarily for this illustration, but the LRDs can be designed for any value of T_{rated}. The IMS and DO devices were modelled using Eq. 7a & 7b, which are valid for neutrally buoyant devices, whereas the TFI device was modelled using Eq. 9a & 9b. The wet weight of the TFI device was set to 8 kN/m, which corresponds to the weight of a 1m-diameter device with rated tension of 2 MN.

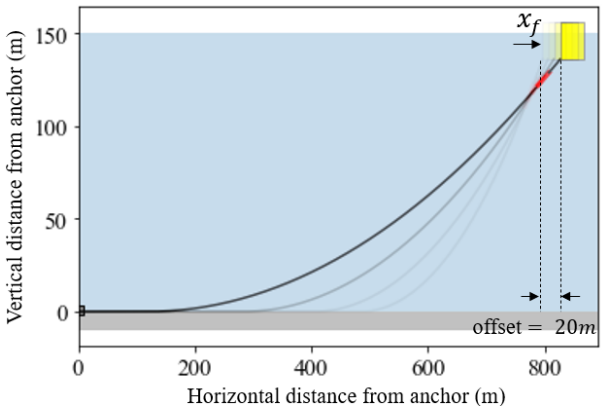

FIGURE 9: 2D PLOT OF MOORING LINE, WITH FAIRLEAD DISPLACED ALONG HORIZONTAL AXIS UP TO AN OFFSET OF 20M

TABLE 5: MOORING SYSTEM PARAMETERS, BASED ON OC4 [16]

Mooring system parameter	Value
Fairlead-seabed vertical dist.	136 m
Unstretched mooring line length inc. LRD	825.35 m
Initial anchor-fairlead distance	796.7 m
Chain mass per unit length	145 kg/m
Chain EA	750 MN

The resulting tension-offset plots are shown in Figures 10, 11 and 12. These are displayed alongside the equivalent full-chain mooring system tension-offset, i.e. a catenary mooring with the same overall line length but no LRD. These show close alignment between the analytical and FE results, with a mean error $< 0.1\%$ and a maximum error across all curves of 0.4%. The maximum error occurs at the gradient change point of the TFI curve, where the fitted stiffness curve does not perfectly match the interpolated curve (Fig. 8). Other general take-away points from the tension-offset profiles are listed below:

- All three LRD moorings show significantly more compliance than the full-chain catenary (i.e. lower gradient of tension-offset), especially at lower offsets where the LRDs operate in their low-stiffness regions. As a result of this increased compliance, the LRD moorings display higher horizontal offsets than the full-chain mooring for the same fairlead tension.
- All three LRDs have exhausted all their extensibility once the fairlead tension is above the rated tension of the device. In practice, this would mean no extension is left to reduce dynamic loads. If these high loads/offsets are expected, an LRD with higher rated tension should be used.
- The extension of the LRDs under the weight of the chain at zero-offset leads to reduced pre-tension of the mooring system. In practice, this could be compensated for by reducing the overall length of line. Due to its self-weight, the TFI device (Fig. 12) shows higher pre-tension than the other LRDs for the same mooring line length.

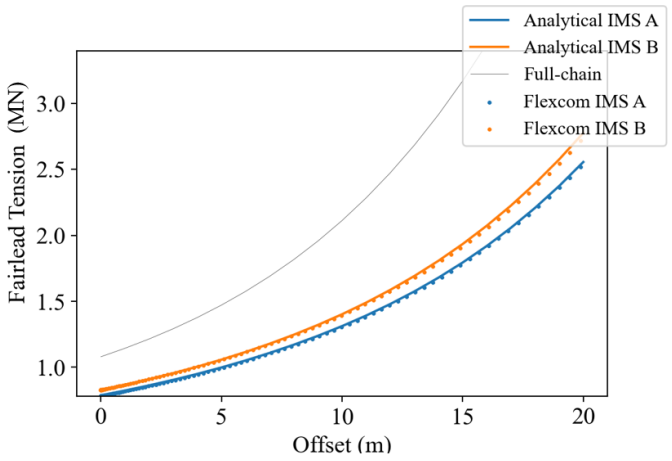

FIGURE 10: TENSION-OFFSET PROFILE FROM ANALYTICAL SOLUTION AND FE SOFTWARE FOR IMS CURVES (CONFIGURATIONS A & B)

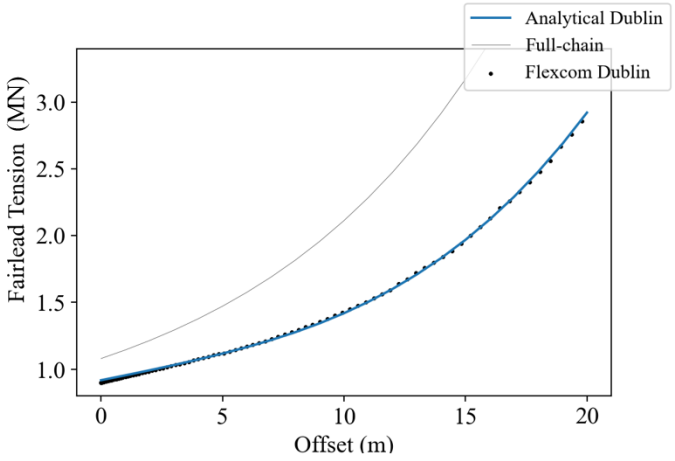

FIGURE 11: TENSION-OFFSET PROFILE FROM ANALYTICAL SOLUTION AND FE SOFTWARE FOR DO CURVE

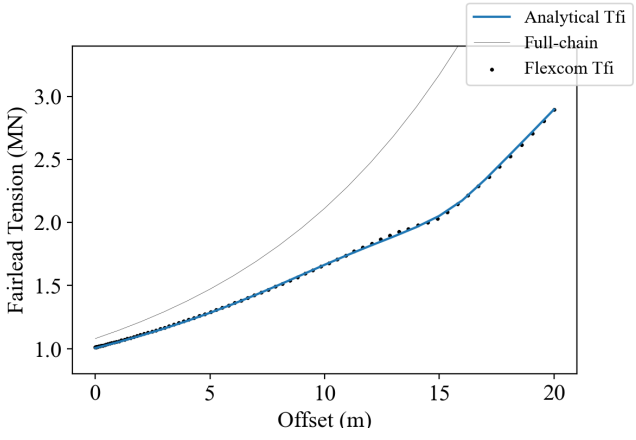

FIGURE 12: TENSION-OFFSET PROFILE FROM ANALYTICAL SOLUTION AND FE SOFTWARE FOR TFI CURVE

5. APPLICATION OF ANALYTICAL MODEL TO LRD DESIGN

5.1 Quasi-static design scenario

Quasi-static design typically involves approximating a mean horizontal environmental force from met-ocean data [9]. This force is applied at the fairlead, and the analytical model can be used to find the fairlead tension and platform offset such that the system is in static equilibrium. For this example, the 50-year horizontal force was set as $F_{env} = 2MN$. Knowing the horizontal fairlead force $H_f = F_{env}$, the vertical force V_f and resulting offset x_f were obtained from eq. 9a & 9b. The 50-year quasi-static fairlead tension $T_{50yr,QS}$ was then calculated from the horizontal and vertical forces. The LRD design parameters could then be adjusted based on the quasi-static offset and fairlead tension.

In particular, two key LRD parameters should be determined at the initial design stage: 1. The rated tension of the device, determined based on the maximum expected load; 2. The maximum extension of the device (i.e., length of the device for spring-like LRDs), determined based on the maximum allowable offset. These parameters are typically found based on iterative dynamic analyses [7], which can be computationally-intensive. This section demonstrates how the analytical model can be used to find a fast initial approximation of the optimal LRD parameters at the quasi-static design stage. This example design scenario is applied to the TFI Seaspring LRD in a catenary mooring system with the physical properties listed in table 5.

5.2 Determining the LRD rated tension

The aim is to determine the suitable T_{rated} for the LRD such that it is not only above the 50-year quasi-static fairlead tension, but also above the 50-year dynamic tensions, to ensure the device can safely operate in the compliant range throughout its design life. Typical quasi-static mooring design approaches require application of a safety factor to the 50-year quasi-static tension to obtain the design tension, with values typically ranging from 1.4 to 2 in relevant design codes [17]. As the LRD is expected to significantly reduce dynamic loads, a low safety factor of 1.4 is used for this example, such that:

$$T_{rated} \geq 1.4 * T_{50yr,QS} \tag{15}$$

To solve this, the analytical model was used to iterate through values of the TFI curve parameter e which is inversely related to T_{rated} (see Eq. 14), starting from a high value of e such that the starting rated tension T_{rated} is equal to the horizontal force F_{env}. All the other curve parameters were fixed to the values shown in Table 4. The fairlead tension, mooring configuration and resulting tension-offset profiles were then computed for each value of e, for the given environmental load until the value of T_{rated} that fits the criterion (Eq. 15) was reached. In this case, the 50-year quasi-static (QS) tension was found to be $T_{50yr,QS} = 2.217MN$, which gives $T_{rated} \geq 3.10MN$ when including the safety factor (Eq. 15). This is depicted graphically in Figure 13. In this case, the value of $T_{50yr,QS}$ is only slightly above the horizontal environmental force F_{env}. This is due to the chain being relatively light, meaning the additional vertical restoring force component at the fairlead is small.

The curve with the lowest rated tension is operating above its rated tension when subjected to the 50-year horizontal load.

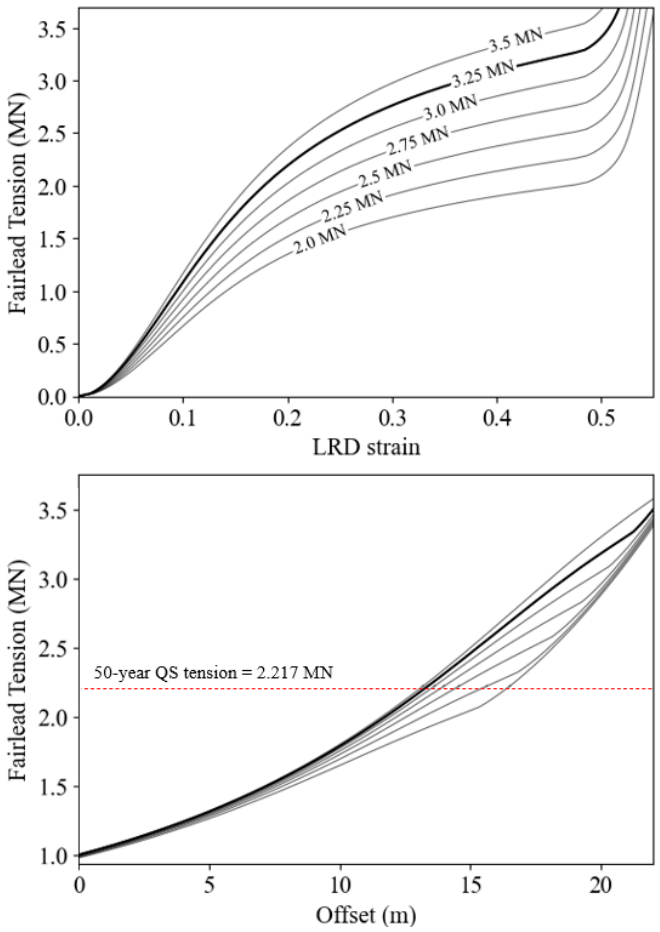

FIGURE 13: TOP: LRD TENSION-STRAIN CURVES FOR 7 VALUES OF T_{rated}; BOTTOM: RESULTING MOORING SYSTEM TENSION-OFFSET PROFILE FOR EACH CURVE. THE CURVE SATISFYING THE DESIGN CRITERION IS SHOWN IN BOLD.

This is visible on the tension-offset profile, with the dashed red line located above the 'kink' in the curve. The curve which satisfies the criterion is operating safely below its rated tension when subjected to the same load, meaning the LRD would be operating in its compliant range as intended. While an even higher rated tension would also be suitable in theory (e.g. 3.5 MN), the resulting tension-offset of the mooring system is stiffer overall, and less effective at reducing loads.

5.3 Determining the LRD length

In the case of a spring-like LRD (e.g. TFI), the length of the device determines its maximum extension, which in turn affects the load reduction potential [18] as well as the resulting platform offset. In the study thus far, LRDs lengths were set such that they exhibit 5 m of extension at the rated strain, i.e. $L_e = 10m$ for the TFI device. For the curve with a rated tension of $T_{rated} = 3.25MN$, the resulting 50-year quasi-static offset is of $T_{50yr,X} = 13.35m$ (can be deduced graphically from Fig. 13). If this is below the maximum quasi-static offset criterion, a longer LRD could be used, for added compliance. As an example, the maximum allowable quasi-static offset is set to 20m. The model was then used to iterate values of L_e, and resulting tension-

offset plots were generated. The optimal length of the LRD is selected by finding the tension-offset profile which is just below the maximum offset for the 50-year tension. This process is depicted in Figure 14, and yields $L_e = 15m$.

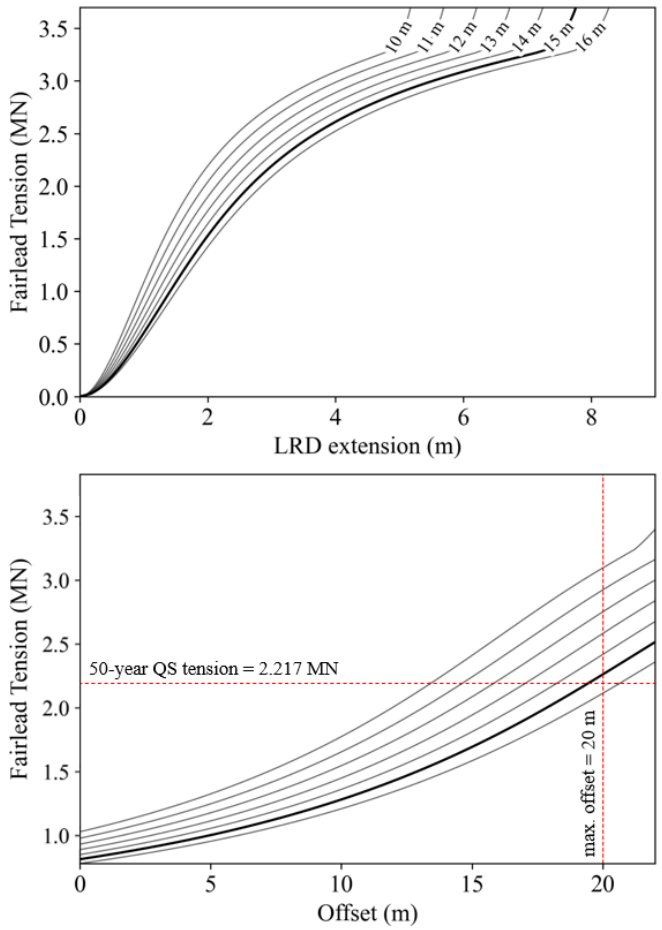

FIGURE 14: TOP: LRD TENSION-EXTENSION CURVES FOR 7 VALUES OF L_e; BOTTOM: RESULTING MOORING SYSTEM TENSION-OFFSET PROFILE FOR EACH CURVE. THE CURVE SATISFYING THE MAXIMUM OFFSET CRITERION IS SHOWN IN BOLD.

6. CONCLUSION

This paper presented an analytical quasi-static tension-offset model of catenary moorings with LRDs with three different non-linear stiffness curves. The model is applicable to any catenary mooring scenario, and is of particular interest for initial FOWT mooring design and analysis. Continuous parameterised equations, defined for the stiffness curves of three different LRDs, were incorporated into the static equations for a multi-segmented catenary mooring. Results from the analytical model, using the continuous equations for the LRD stiffness, match closely with results of a commercial FE model, which uses piece-wise interpolation of user-defined LRD stiffness cruves. The analytical model has been packaged into an executable function as well as an associated web application, which enables visualisation of the mooring geometry and tension-offset profiles for any input LRD and mooring design parameters [15].

The effectiveness of the analytical model has also been demonstrated here through an example quasi-static design scenario, and was used to find an initial LRD design for a given 50-year environmental load. By determining the optimal stiffness curve, the LRD was ensured to operate below its rated tension, and by finding the optimal LRD length, it satisfied the maximum offset criterion while maintaining maximum compliance. This design approach yields quasi-instantaneous results, and could provide an efficient starting point for subsequent dynamic analyses.

ACKNOWLEDGMENTS

This work forms part of the activities of the Royal Academy of Engineering Chair in Emerging Technologies Centre of Excellence for Intelligent & Resilient Ocean Engineering (www.southampton.ac.uk/iroe), based at the University of Southampton. Susan Gourvenec is supported by the Royal Academy of Engineering under the Chairs in Emerging Technologies scheme. Adam Sobey is supported by the Alan Turing institute.

REFERENCES

[1] Burges Salmon. "Floating Wind – Challenges and Opportunities for a Buoyant Technology,." *Burges Salmon - News & Insight* URL https://www.burges-salmon.com/news-and-insight?Sector+expertise=Energy+Power+and+Utilities.

[2] COREWIND. "D1.2 Design basis." URL https://corewind.eu/wp-content/uploads/files/publications/COREWIND-D1.2-03-Design-Basis.pdf.

[3] COREWIND. "D3.1 Review of the state of the art of dynamic cable system design." URL https://ec.europa.eu/research/participants/documents/downloadPublic?documentIds=080166e5cca0f37e&appId=PPGMSl.

[4] Cruz, J. and Mairead, A. "Floating Offshore Wind Energy : The Next Generation of Wind Energy." *Green Energy and Technology*. 2016. Springer. URL http://search.ebscohost.com/login.aspx?direct=true&db=nlebk&AN=1282129&site=ehost-live.

[5] Harrold, M., Thies, P., Johanning, L., Newsam, D., Checkley, M. and Bittencourt Ferreira, C. "Dynamic load reduction and station keeping mooring system for floating offshore wind." *ASME 2018 1st International Offshore Wind Technical Conference*. 2018. American Society of Mechanical Engineers Digital Collection.

[6] Dublin Offshore. "Load Reduction Device (LRD) – How it works." URL https://www.dublinoffshore.ie/media/pages/technology/6f4e7419f6-1635594571/how-it-works.pdf.

[7] Lozon, E., Hall, M., McEvoy, P., Kim, S. and Ling, B. "Design and Analysis of a Floating-Wind Shallow-Water Mooring System Featuring Polymer Springs." *International Offshore Wind Technical Conference (IOWTC2022)*. 2022.

[8] WFO. "Mooring Systems for Floating Offshore Wind: Integrity Management Concepts, Risks and Mitigation,." *World Forum Offshore Wind 2022 e.v.* URL https://wfo-global.org/?jet_download=5751.

[9] Ma, K., Luo, Y., Kwan, T. and Wu, Y. "Mooring System Engineering for Offshore Structures." Ma, K., Luo, Y., Kwan, T. and Wu, Y. (eds.). *Chapter 15 - Mooring for floating wind turbines*. Gulf Professional Publishing (2019): pp. 299–315. DOI https://doi.org/10.1016/B978-0-12-818551-3.00015-6. URL https://www.sciencedirect.com/science/article/pii/B9780128185513000156.

[10] Oppenheim, B and Wilson, P. "Static 2-D Solution of a Mooring Line of Arbitrary Composition in the Vertical and Horizontal Operating Modes." *International shipbuilding progress* Vol. 29 (1982): pp. 142–153.

[11] Jonkman, J. "Dynamics modeling and loads analysis of an offshore floating wind turbine." Technical Report No. NREL/TP-500-41958. National Renewable Energy Lab (NREL), Golden, CO (United States). 2007. URL https://www.nrel.gov/docs/fy08osti/41958.pdf.

[12] McEvoy, P. and Johnston, E. "Polymer Mooring Component for Offshore Renewable Energy." *OTC Offshore Technology Conference*, Vol. Day 3 Wed, May 08. 2019. DOI 10.4043/29587-MS. URL https://onepetro.org/OTCONF/proceedings-pdf/19OTC/3-19OTC/D031S033R004/1986721/otc-29587-ms.pdf.

[13] Kelley, C. T. "Solving Nonlinear Equations with Newton's Method.": pp. 57–83. 2003. Society for Industrial and Applied Mathematics. DOI 10.1137/1.9780898718898.ch3. URL https://epubs.siam.org/doi/pdf/10.1137/1.9780898718898.ch3.

[14] Ramberg, W. and Osgood, W. "Description of stress-strain curves by three parameters." Technical Report No. 902. National Advisory Committee for Aeronautics. 1943.

[15] Festa, Oscar. "Quasi-static LRD mooring model." (2023). DOI 10.5281/zenodo.7794703. URL https://doi.org/10.5281/zenodo.7794703.

[16] Robertson, A., Jonkman, J., Vorpahl, F., Popko, J., W.and Qvist, Frøyd, Lars, Chen, X., Azcona, J., Uzunoglu, Emre, Guedes Soares, Carlos, Luan, Chenyu, Yutong, H., Pengcheng, Feng, Yde, Anders, Larsen, Torben, Nichols, James, Buils, R., Lei, L., Nygard, T. and Guerinel, Matthieu. "Phase II Results Regarding a Floating Semisubmersible Wind System." *Offshore Code Comparison Collaboration Continuation Within IEA Wind Task 30*. 2014. DOI 10.13140/2.1.2822.9121. URL https://www.nrel.gov/docs/fy14osti/61154.pdf.

[17] Brevik, S. and Kovesdi, B. "Modifications to DNV Mooring Code (POSMOOR) and Their Consequences." *Proceedings of the 17th International Conference on Offshore Mechanics and Arctic Engineering*, Vol. 1: pp. 169–177. 1998. American Society of Mechanical Engineers.

[18] Festa, O., Gourvenec, S. and Sobey, A. "Proxy model for the design of extensible floating offshore wind turbine mooring systems." *In Proc. 32nd International Symposium on Ocean and Polar Engineering (ISOPE), June 5 – 10 (virtual)*. 2022. URL https://eprints.soton.ac.uk/457473/.

[19] Davidson, J. and Ringwood, J. "Mathematical Modelling of Mooring Systems for Wave Energy Converters—A Review." *Energies* Vol. 10 No. 5. DOI 10.3390/en10050666. URL https://www.mdpi.com/1996-1073/10/5/666.

[20] Festa, O., Gourvenec, S. and Sobey, A. "Comparative parametric analysis of extensible catenary moorings for floating offshore wind turbines." *2021 CORE - Glasgow*. 2021. URL https://eprints.soton.ac.uk/457472/.

[21] Kwan, C.T. and Bruen, F.J. "Mooring Line Dynamics: Comparison of Time Domain, Frequency Domain, and Quasi-Static Analyses." *OTC Offshore Technology Conference*. 1991. DOI 10.4043/6657-MS. URL https://onepetro.org/OTCONF/proceedings-pdf/91OTC/All-91OTC/OTC-6657-MS/1997242/otc-6657-ms.pdf. OTC-6657-MS.